Nonlinear Integrable Optics (NIO) in IOTA Run 2

Alexander Valishev,[1,*] Nikita Kuklev,[2] Alexander Romanov,[1]
Giulio Stancari,[1] and Sebastian Szustkowski[3]

[1]*Fermi National Accelerator Laboratory*

[2]*University of Chicago*

[3]*Northern Illinois University*

CONTENTS

* valishev@fnal.gov

I. INTRODUCTION

The overarching goals of the Nonlinear Integrable Optics (NIO) experiments in IOTA are i) the demonstration of a practical implementation of the NIO concept [1] in a real accelerator [2]; ii) the study of fundamental aspects of stability of such lattices to imperfections; and iii) demonstration of benefits of NIO lattices in high-intensity synchrotrons [3].

The NIO research program in IOTA is comprised of two major parts:

1. Studies with electron beams with focus on the aspects of single-particle betatron dynamics, allowed by the properties of 100–150 MeV electron beams in IOTA: the suppressed collective effects, and the small transverse size of electron beam compared to the available machine aperture. These factors mean that the transverse motion of an electron bunch as observed by the machine beam position monitors (BPM) can be effectively treated as the motion of a single particle.

2. Studies with proton beams, which deal with the physics of space-charge dominated beams in strongly nonlinear lattices. The 2.5 MeV kinetic energy proton beam in IOTA will be strongly affected by the space-charge forces. Additionally, the long proton bunches allow for the investigation of coherent intra-beam motion and the impact of NIO on coherent beam stability. The demonstration of practical benefits for high-intensity and high-brightness hadron beams is the ultimate goal of IOTA NIO research program.

The studies in IOTA/FAST Run 2 dealt with the first part of the NIO research. Initial NIO experiments in Run 1 [4–6] demonstrated that a record-high nonlinear amplitude-dependent betatron tune shift can be attained in IOTA with the use of NIO lattice. However, the status of IOTA lattice tuning and, most importantly, of the BPM system prevented the implementation of the full-breadth research program in Run 1. Extensive machine upgrades during the 2019 summer shutdown enabled a better quality research program in Run 2.

II. NIO EXPERIMENTS IN IOTA RUN 2

The Run 2 plan included three types of NIO lattices:

- System with one invariant of motion, also referred to as the Quasi-Integrable or Hénon-Heiles-type system, implemented with a quasi-continuous octupole focusing channel [7, 8], denoted below as QI.

- System with two invariants of motion, also called the Danilov-Nagaitsev system [1], implemented with a quasi-continuous nonlinear elliptic-potential focusing channel, denoted as DN.

- Quasi-Integrable system with one invariant of motion similar to QI, but implemented with a version of symplectic integrator based on a small number of discrete octupole magnets [9], further referred to as SIQIS.

These implementations largely rely on similar machine configurations, methods of measurement, data acquisition, and can be executed concurrently. This motivated combining them into one research proposal. The premature end of IOTA/FAST Run 2 due to the accelerator shutdown caused by the COVID-19 pandemic prevented the study of the SIQIS configuration. The QI and DN experiments collected relevant data. However, the full program of studies was not executed.

The NIO experiments in Run 2 sought to demonstrate that

1. Large values of amplitude-dependent nonlinear tune shift can be achieved without reduction of dynamical aperture.

2. Theoretically predicted invariants of the motion, calculated from measured turn-by-turn bunch coordinates, are conserved over the course of observation.

3. The NIO systems are substantially stable to perturbations and imperfections of implementation, such as the errors in β-functions and phase advances of the T-insert, dispersion, alignment errors, natural machine nonlinearities, and artificially introduced nonlinearities (sextupoles).

Accordingly, the study plan was logically divided into 3 phases addressing the following main goals:

1. Goal 1: Demonstration of the magnitude of nonlinear detuning without degradation of dynamical aperture in agreement with predictions for QI and DN experiments.

2. Goal 2: Demonstration of the invariant conservation for QI and DN experiments.

3. Goal 3: Systematic studies of integrability conservation in all three systems: variation of sextupole strengths, Q_0 for the QI option (with particular interest towards values near 1/4 integer resonance), and study of the effect of integer resonance on dynamics in the DN system.

In the proposed plan, we estimated that 12 8-hour shifts were required to fulfill this program. The main risk associated with the proposed schedule was believed to be related to the machine performance at the beam energy of 100 MeV and to the possible need to commission 150-MeV operations. This is due to significant intrabeam scattering (IBS) effects at the beam currents needed for optimal BPM sensitivity. IBS manifests itself in two ways: i) increased bunch momentum spread, which in turn leads to faster decoherence of the dipole oscillations and ii) increased bunch transverse size, leading to stronger nonlinear decoherence. The precise reconstruction of turn-by-turn phase space coordinates requires a large number of turns in the recorded signals. Simulations suggested that a reduction of the relative momentum spread from Run 1 values (about 2×10^{-3}) by raising the beam energy to 150 MeV would produce a marked improvement of the turn-by-turn signal quality.

In all, 19 shifts were allocated in Run 2 for NIO studies by the IOTA/FAST run coordination team. It should be noted that this balance includes data taking for the NL-OMC experiment []. Most importantly, a significant fraction of time in the NIO shifts was used for hardware commissioning, specifically of the BPM system. The BPM system became fully operational only during the last two weeks of the run. This and the COVID-19 shutdown substantially affected the outcome of Run 2 for NIO experiments: of the three formulated goals, only Goal 1 was accomplished fully. Limited data was collected in pursuit of Goal 2, and Goal 3 was not addressed.

In this document, we report on the completed measurements for each experiment and present brief summaries of the results. We also discuss the outlook for further work and necessary improvements. Two peer-reviewed publications are currently being prepared summarizing the accomplishments of the DN and QI NIO experiments.

III. EXPERIMENTAL METHODS

All versions of the NIO lattices in IOTA rely on the so-called T-insert concept [10], where the nonlinear focusing is implemented in a relatively short straight section of the machine circumference, while the remainder of the ring can be represented by a thin axially symmetric focusing lens (T-insert). In the case of IOTA (Figure 1), the two sections dedicated to nonlinear focusing magnets are BR for the DN magnet [11], and BL for the octupole string — a sequence of 17 octupole magnets of equal lengths [8]. Both sections have a length of 1.8 m.

The nominal IOTA NIO optics is mirror-symmetric with respect to the L-R axis and has the betatron tunes $Q_x = Q_y = 5.3$ (phase advance of 5 in the T-insert and $Q_0 = 0.3$ in each of the nonlinear straights, see also Figure 2). This corresponds to a β-function of 0.65 m in the middle of the BL and BR sections. The lattice can be tuned to have Q_0 between approximately 0.25 and 0.35 without the loss of mirror symmetry.

All of the IOTA NIO concepts rely on a precise tuning of the optics, and the project strives to achieve better that 1% precision in β-functions and better than 0.001 precision in horizontal and vertical phase advances through the BL and BR sections [12]. An important optics design parameter is the momentum compaction α_p, which was maximized to be approximately 0.07 in order to minimize the coupling between the transverse and longitudinal degrees of freedom.

Upgrades of the IOTA ring during the 2019 shutdown aimed to improve the lattice control precision:

- The stability of the main bending dipole power supply was improved, reducing the horizontal orbit jitter.
- Fringe field correctors were installed on all bending dipole magnets to alleviate the orbit sagitta.
- The precision and dynamic range of orbit measurement with the BPM system was improved.
- The kicked-beam turn-by-turn beam position measurement was significantly improved.

The aforementioned measures led to a marked improvement in the machine lattice model reconstruction. Two methods were used to tune the IOTA lattice: the slower LOCO tool provided the baseline focusing configuration, which was then fine-tuned on a day-to-day basis using turn-by-turn kicked beam tune and phase adjustments. We estimate that the β-functions were within 3% of the design values. The errors in betatron tune and phase advance through BL and BR were kept below 2×10^{-3}.

The other essential machine tuning factor for NIO experiments was the magnet alignment and orbit centering through the nonlinear insertions. The alignment and centering of the DN magnet had not changed since Run 1: the individual deviations from the beam axis of the centers of the 18 magnetic element were under 100 μm both horizontally and vertically, with a standard deviation below 50 μm. The alignment of the octupole magnets in Run 2 proved difficult due to a combination of factors. We estimate that the offsets of individual octupole centers from the beam orbit had a standard deviation of 0.5 mm.

In terms of the measurement methods, the experiments relied on the reconstruction of transverse phase-space dynamics of a single bunch after betatron oscillations were induced by a transverse single-turn kicker pulse. For Run 2, both the horizontal and vertical full-aperture kickers synchronized with the BPM data acquisition were commissioned (in contrast to Run 1, when the horizontal kick was of very small amplitude and could not be varied). The turn-by-turn horizontal and vertical beam centroid positions were recorded synchronously at all 21 BPMs for a minimum of 2000 turns.

In addition to the BPM data, beam images were collected with the use of the synch-light camera system, at a rate of up to 20 frames/s.

During Run 2, we used specialized software tools for tuning and data collection:

- 6DSim: IOTA orbit and lattice tuning, nonlinear magnet orbit centering.
- pyIOTA: control of the beam injection, kicks, turn-by-turn data collection, preliminary analysis.
- Other: scripts in ACL and Python for small tasks, such as timing of the machine-protection system (MPS), BPM triggering, etc.

IV. RESULTS OF EXPERIMENT QI

The QI experiment makes use of 17 discrete octupoles to approximate a continuous potential of a Hamiltonian with one invariant of motion, the Hamiltonian itself. This system is also known as a Hénon-Heiles system of octupole type. Over the summer of 2019, the octupole insert was completely disassembled and underwent rotating coil measurements at Fermilab's magnet test facility to verify field quality. The insert was reassembled with best magnets in middle positions, as they run at the highest currents. Alignment was performed using the laser pinhole method, in the same way as in Run 1. In addition, the alignment was verified with a precisely machined rod, with a length of 1 m and a diameter 100 μm smaller than the nominal bore size of 27.84 mm (1.096 in). This rod successfully cleared the full insert, indicating good mechanical alignment. However, subsequent beam-based measurements were in strong disagreement, as noted previously. The causes are still under investigation.

Changing the strength of the octupole insert does not affect the small-amplitude tune of the system, whereas the amplitude-dependent detuning varies linearly with octupole strength. The experimental configurations were typically labelled by the current in the central (strongest) octupole magnet. This value can be converted into an equivalent t-value for comparison with the DN case. In Run 2, the best configuration, i.e. a dynamic aperture near the physical limit, was expected at the octupole current of 1.0 A. Many other set points were explored as well.

Two representative Run 2 data sets are shown in Figure 3. The observed detuning was in agreement with simulations. At the dynamic aperture limit, a tune shift of 0.04 was achieved.

Simulations showed that the limiting DA factor was not the insert itself, but the strong sextupole correction that had to be used to lower chromatic decoherence. Installation of all 12 planned sextupole magnets in IOTA is expected to resolve this limitation.

V. RESULTS OF EXPERIMENT DN

The DN experiment makes use of the specially designed nonlinear magnet [11] to implement a Hamiltonian system that possesses two invariants of the motion: the Hamiltonian itself, similarly to the QI case, and a second function quadratic in momenta [1]. The nonlinear magnet, designed and built by RadiaBeam Technologies, was installed in the BR section of IOTA.

The magnet bore creates the smallest aperture restriction of the ring: $\pm$5.3 mm vertically and $\pm$3.2 mm horizontally at the mid-point of the BR straight. The magnet comprises 18 individually shaped and independently powered sections. At the beam energy of 100 MeV, the dimensionless t strength can be varied

between -1 and $+1$. At the t value of 0.5, the vertical small-amplitude fractional betatron tune reaches the value 0 — the magnet is capable of creating conditions for crossing the integer resonance line.

An important feature of the DN case is that the small-amplitude betatron tunes are a function of t, unlike the octupole-driven QI case. Figure 4a shows the predicted dependence of Q_x and Q_y on the magnet strength, compared to the values measured in Run 1.

The maximum predicted nonlinear amplitude-dependent tune shift is 0.08 at $t = 0.43$ and 0.11 at $t = 0.48$. During Run 1, a tune shift 0.053 was achieved with a nonlinear potential strength of $t = 0.43$. However, beam loss was observed. Figure 4b shows the predicted DN experiment performance as well as the Run 1 data.

During Run 2, extensive measurements were done at three strengths: $t = 0.218$, $t = 0.363$, and $t = 0.420$, in both nominal and perturbed configurations. Data in nominal configurations and ideal lattice simulations (using code OCELOT) are shown in Figures 5–7. The experiments at $t = 0.420$ showed significant beam loss and had quality issues that prevented a direct comparison with Run 1. However, for $t = 0.363$, a large tune shift of 0.08 was achieved. (This value is similar to what was achieved in Run 1 at $t = 0.43$.) These larger tune shifts indicate that lattice tuning had been significantly improved, approaching the required conditions for the DN nonlinear integrable system.

In Run 2, we recorded the beam current as a function of the value of the strength t to study the effect of resonances on the nonlinear integrable system. The scans in the t parameter were similar to those shown in Figure 4a. The studies were extended beyond the value $t = 0.5$ (integer crossing). Figure 8a shows the nonlinear potential strength being ramped from $t = 0$ to $t = 0.60$ in 100 s, along with the corresponding beam current. At $t = 0.146$, the beam was close to third- and fourth-order resonances. Remarkably, the beam crossed the integer resonance at $t = 0.5$. Figure 8b shows a faster ramp, from $t = 0$ to $t = 0.5$ in 15 s, along with the corresponding beam current. The beam was left on the integer resonance at $t = 0.5$ for 110 s. Afterwards, the nonlinear magnet was turned off.

To study the transverse profile of the beam beyond the integer resonance, we recorded 1 s exposures with the synchrotron-light diagnostic cameras. Remarkably, in agreement with the theoretical predictions, two stable beamlets were observed when the nonlinear strength was increased beyond $t = 0.5$. With increasing t-strength, the distance between the two beamlets increased nonlinearly up to $t = 0.90$, when the beamlets hit the mechanical aperture of the beam pipe. Figures 9a and 9b show the images of the beamlets at $t = 0.55$ and $t = 0.88$, respectively.

VI. DATA AND DOCUMENTATION

The group maintains a project web site [13] with descriptions and resources on NIO experiments, including the QI and DN subprojects.

The progress of the studies was documented in the FAST electronic logbook: www-bd.fnal.gov/Elog/?orLogName=FAST.

Experimental data, including turn-by-turn BPM signals, is stored on the shared network drive N: at `\\Beamssrv1\nmlscrf.bd\ControlRoom\nkuklev`. The data will be backed up to the dedicated IOTA network shared drive `\\Beamssrv1\iota-fast.bd\Data`, together with new data from future runs.

The IOTA lattice files and data collected during LOCO measurements were saved in the Y: drive of the control room consoles at `\\Beamssrv1\console_temp\aromanov\_expData`.

Source code for 6DSim is not publicly available. A current compiled version can be found on the control

room consoles at `\\Beamssrv1\console_temp\aromanov\bin`.

The pyIOTA framework is available as open-source software under GPLv3 [14].

VII. AUTHOR ROLES

Alexander Valishev (Principal Investigator), scientist: experiment design and modeling, machine tuning, data acquisition, data analysis. *Nikita Kuklev*, graduate student: experiment modeling, data acquisition, sync-light optics, data analysis. *Alexander Romanov*, scientist: lattice modeling, machine tuning, sync-light optics. *Giulio Stancari*, scientist: beam instrumentation, data analysis. *Sebastian Szustkowski*, graduate student: experiment modeling, data acquisition, data analysis, software for lattice tuning.

VIII. ACKNOWLEDGMENTS

This manuscript has been authored by Fermi Research Alliance, LLC under Contract No. DE-AC02-07CH11359 with the U.S. Department of Energy, Office of Science, Office of High Energy Physics. Work was also supported by the DOE General Accelerator Research and Development (GARD) Program and by the U.S. National Science Foundation under award PHY-1549132 through the Center for Bright Beams at the University of Chicago.

FIGURES

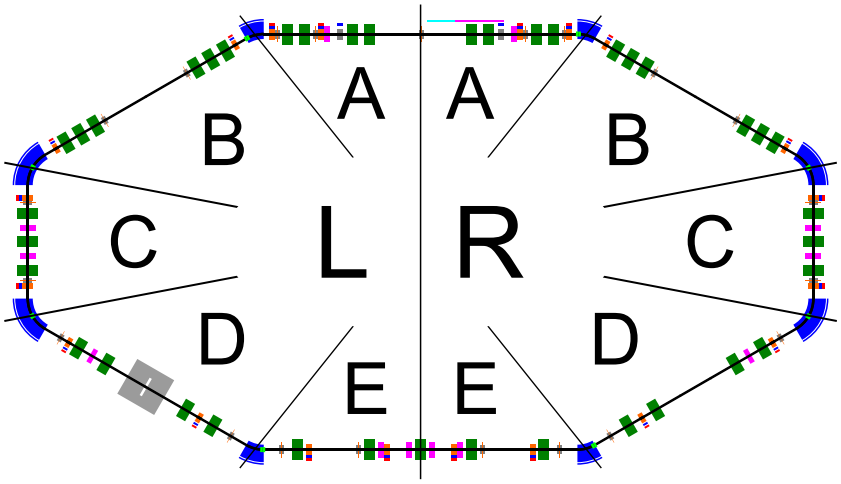

FIG. 1: IOTA layout and naming convention.

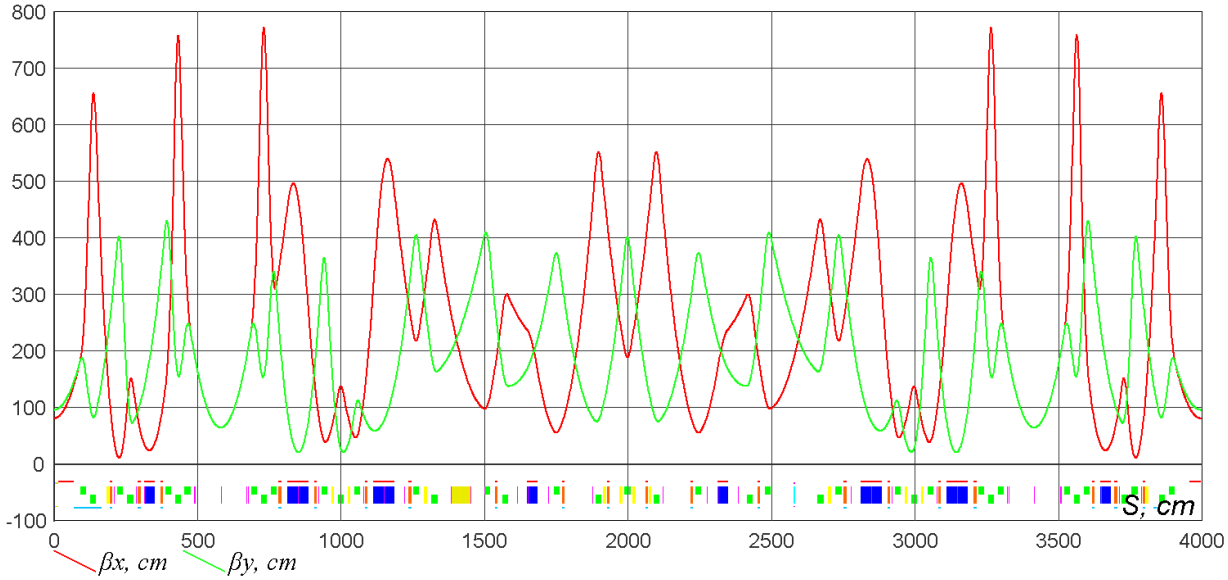

FIG. 2: Beta-functions for the nominal IOTA NIO optics. The origin corresponds to the injection point between the A sections of Figure 1. The longitudinal coordinate S increases going clockwise.

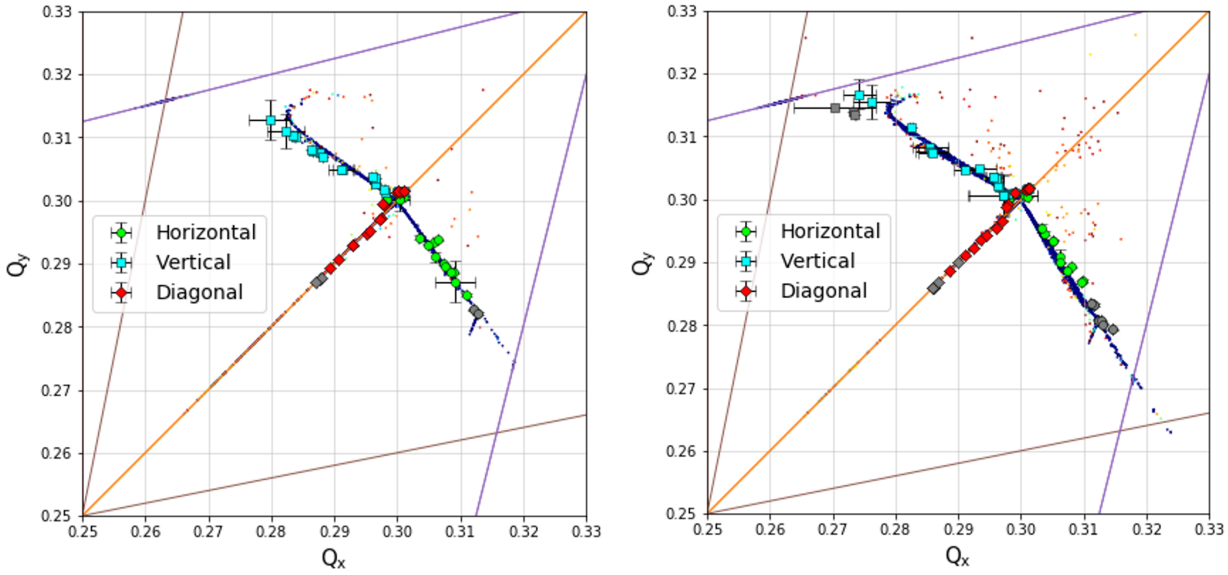

(a) Nominal QI distribution at 1.0 A.

(b) Flat (non-integrable) profile at 0.25 A.

FIG. 3: QI data from Run 2. The green, cyan and red points represent the measured tunes for different values of the horizontal, vertical and diagonal single-turn transverse kicks. Gray points denote rejected data. The small dots are the results of numerical tracking simulations.

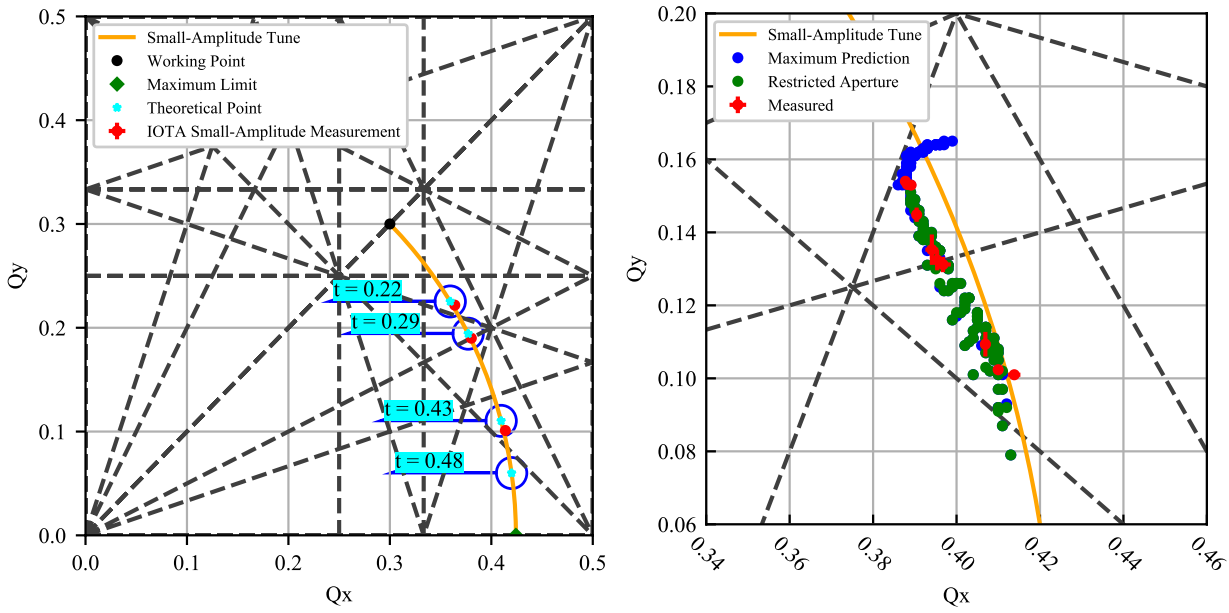

(a) Small-amplitude tunes as function of nonlinear magnet strength t: theoretical predictions (yellow line), numerical simulations (cyan points) and measured data (red points).

(b) Tunes as function of betatron amplitude for nonlinear magnet strength $t = 0.43$. Simulations were done in MAD-X for the nominal case (blue points) and taking into account the restricted IOTA aperture in Run 1 (green points). The red points represent the measured values.

FIG. 4: Simulations and data for experiment DN in Run 1.

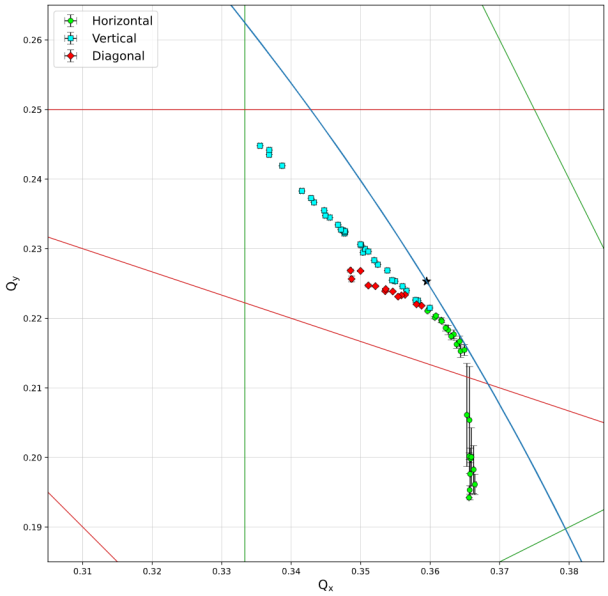

(a) Measured tunes for different amplitudes of the horizontal (green), vertical (cyan) and diagonal (red) transverse kicks.

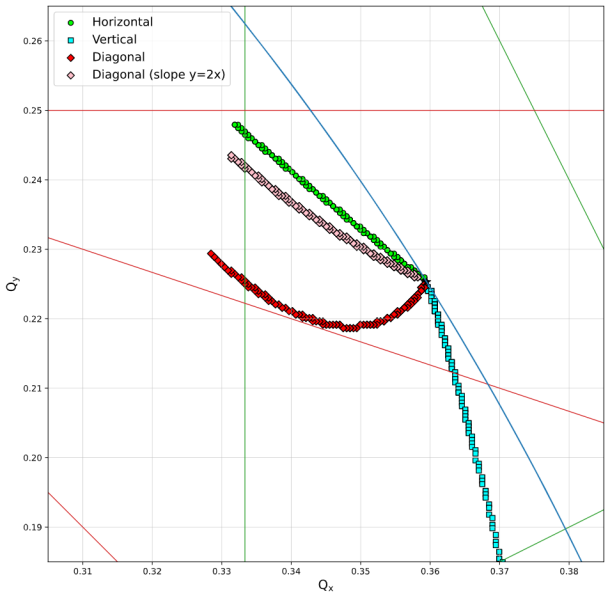

(b) Simulated tune distributions for horizontal, vertical and diagonal kicks (with 2 different ratios of horizontal to vertical amplitudes).

FIG. 5: Data and simulations for experiment DN at $t = 0.218$ in Run 2.

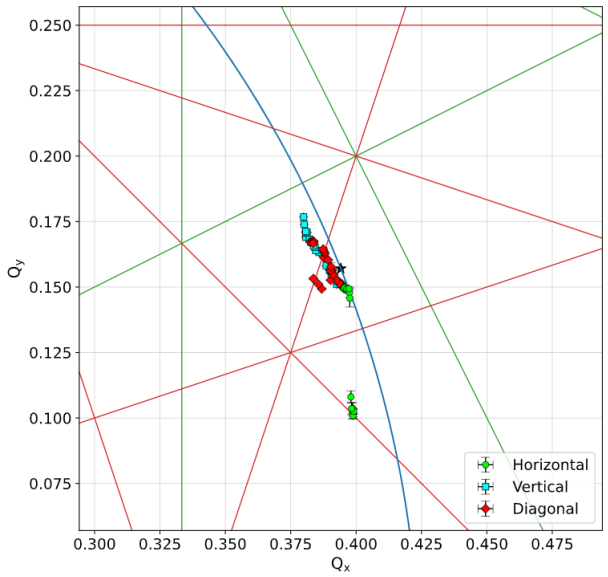

(a) Measured tunes for different amplitudes of the horizontal (green), vertical (cyan) and diagonal (red) transverse kicks.

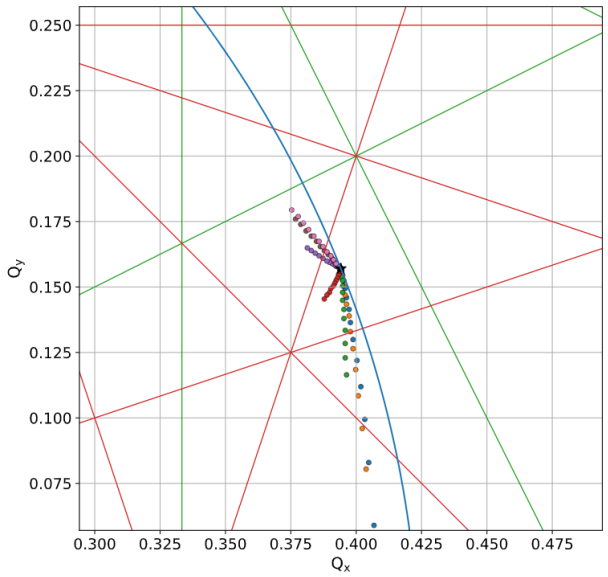

(b) Simulated tune distributions for horizontal, vertical and diagonal kicks (with several different ratios of horizontal to vertical amplitudes, see Figure 6c below).

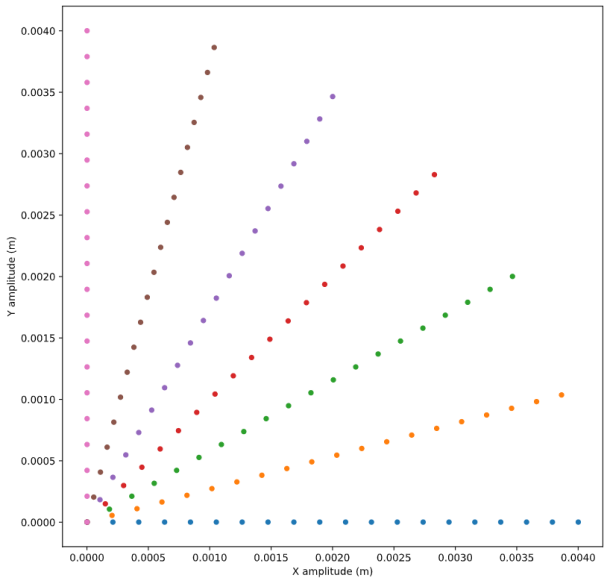

(c) Range of horizontal and vertical kick amplitudes used in the simulations above (Figure 6b).

FIG. 6: Data and simulations for experiment DN at $t = 0.363$ in Run 2. The spacing in tune space of the blue and orange points indicates strong detuning.

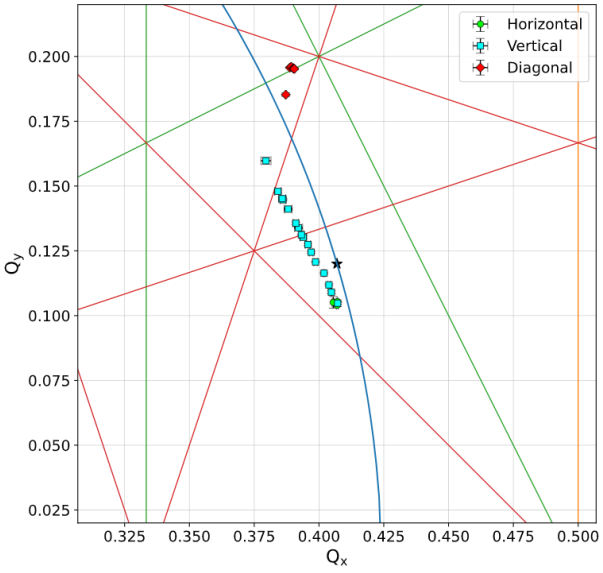

(a) Measured tunes for different amplitudes of the horizontal (green), vertical (cyan) and diagonal (red) transverse kicks.

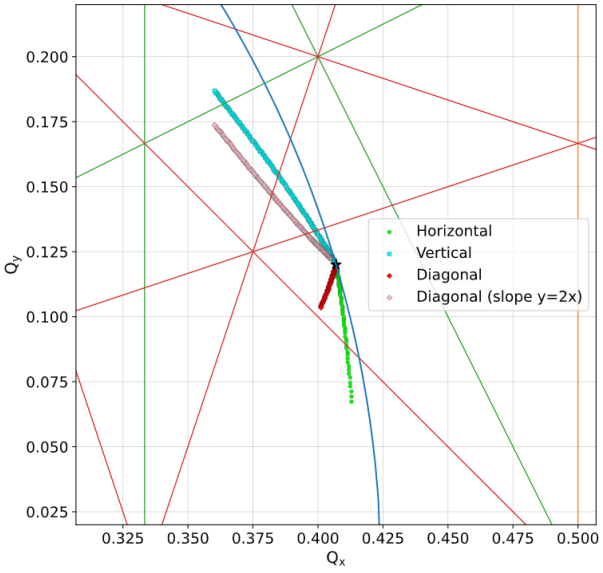

(b) Simulated tune distributions for horizontal, vertical and diagonal kicks (with 2 different ratios of horizontal to vertical amplitudes).

FIG. 7: Data and simulations for experiment DN at $t = 0.420$ in Run 2. The diagonal measurements had incorrect linear optics settings and are only reported for completeness. During the horizontal scan, the beam was lost after the 3rd kick, so only small amplitude data is available.

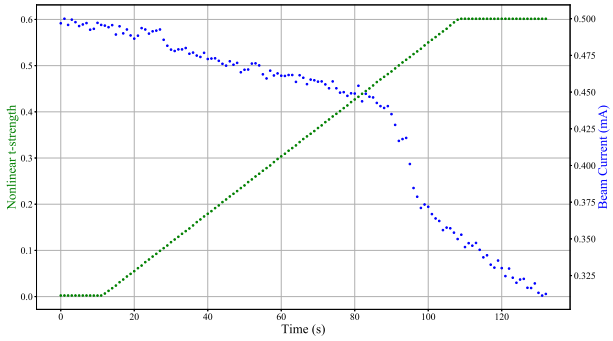

(a) Beam current and nonlinear t-strength during the slow ramp from $t = 0$ to $t = 0.60$.

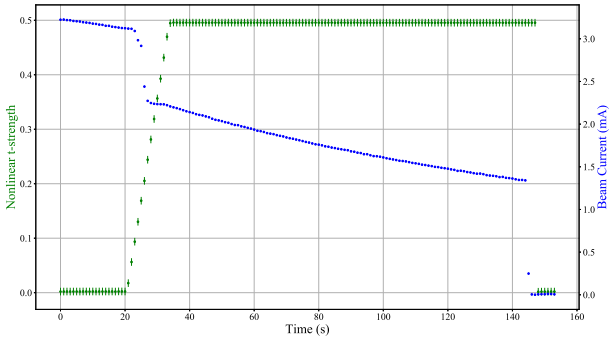

(b) Beam current and nonlinear t-strength during the fast ramp from $t = 0$ to $t = 0.50$.

FIG. 8: Experiment DN in Run 2: Beam current during scans of the nonlinear strength t across resonances.

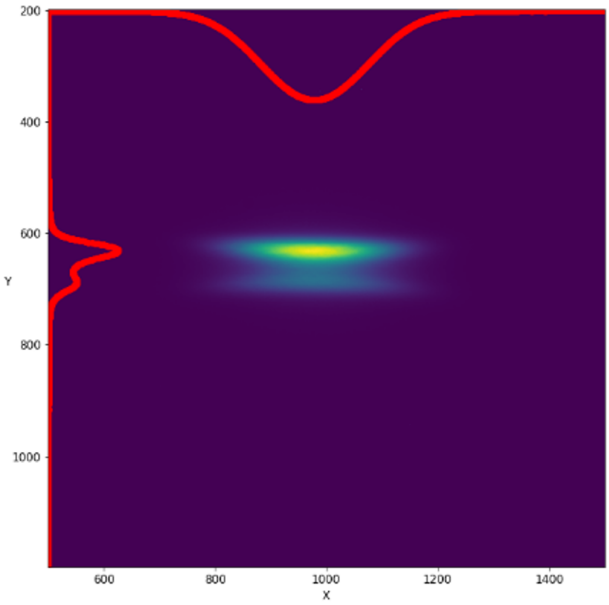

(a) $t = 0.55$

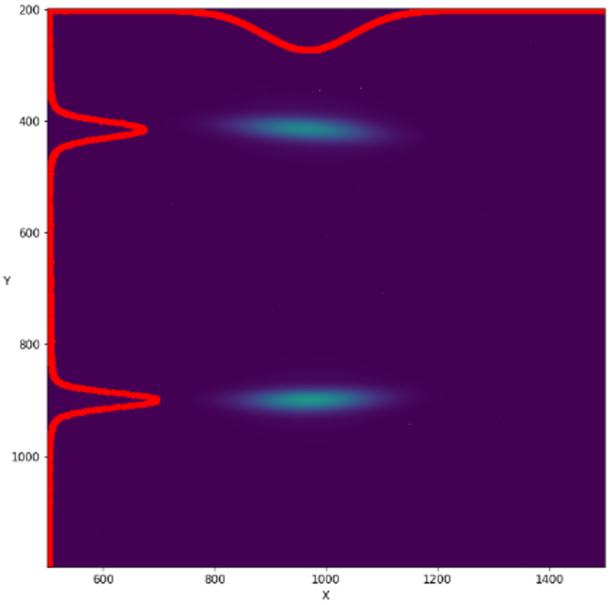

(b) $t = 0.88$

FIG. 9: Images recorded by one of the synchrotron-light diagnostic cameras (M2L) when the strength of the nonlinear magnet was increased beyond $t = 0.5$.

[1] V. Danilov and S. Nagaitsev, Nonlinear accelerator lattices with one and two analytic invariants, Phys. Rev. ST Accel. Beams **13**, 084002 (2010).

[2] S. Antipov, D. Broemmelsiek, D. Bruhwiler, D. Edstrom, E. Harms, V. Lebedev, J. Leibfritz, S. Nagaitsev, C. S. Park, H. Piekarz, P. Piot, E. Prebys, A. Romanov, J. Ruan, T. Sen, G. Stancari, C. Thangaraj, R. Thurman-Keup, A. Valishev, and V. Shiltsev, IOTA (Integrable Optics Test Accelerator): Facility and experimental beam physics program, JINST **12** (3), T03002.

[3] S. Nagaitsev, A. Valishev, and V. Danilov, Nonlinear optics as a path to high-intensity circular machines, in *Proceedings of the 46th ICFA Advanced Beam Dynamics Workshop on High-Intensity and High-Brightness Hadron Beams (HB2010)* (2010) pp. 676–680.

[4] N. Kuklev, Y. K. Kim, S. Nagaitsev, A. L. Romanov, and A. Valishev, Experimental demonstration of the Hénon-Heiles quasi-integrable system at IOTA, in *Proceedings of the 10th International Particle Accelerator Conference (IPAC19)* (2019) pp. 386–389.

[5] S. Szustkowski, A. L. Romanov, A. Valishev, S. Chattopadhyay, and N. Kuklev, Nonlinear tune-shift measurements in the Integrable Optics Test Accelerator, in [15], p. TUZBB6.

[6] A. L. Romanov *et al.*, Recent results and opportunities at the IOTA facility, in [15], p. WEXBA2.

[7] S. A. Antipov, S. Nagaitsev, and A. Valishev, Single-particle dynamics in a nonlinear accelerator lattice: Attaining a large tune spread with octupoles in IOTA, JINST **12** (04), P04008.

[8] S. A. Antipov, A. Valishev, S. Wesseln, K. Carlson, and R. Castellotti, Design of octupole channel for Integrable Optics Test Accelerator, in *Proceedings of the 7th International Particle Accelerator Conference (IPAC16)* (2016) pp. 1731–1733.

[9] S. S. Baturin, Hamiltonian preserving nonlinear optics, arXiv:1908.03520 [physics.acc-ph] (2019).

[10] A. Valishev, S. Nagaitsev, V. Kashikhin, and V. Danilov, Ring for test of nonlinear integrable optics, in *Proceedings of the 2011 Particle Accelerator Conference (PAC11)* (2011) pp. 1606–1608.

[11] F. H. O'Shea, R. Agustsson, Y. C. Chen, E. Spranza, D. W. Martin, and J. D. McNevin, Non-linear magnetic inserts for the Integrable Optics Test Accelerator, in *Proceedings of the 6th International Particle Accelerator Conference (IPAC15)* (2015) pp. 724–727.

[12] A. Romanov, G. Kafka, S. Nagaitsev, and A. Valishev, Lattice correction modeling for Fermilab IOTA ring, in *Proceedings of the 5th International Particle Accelerator Conference (IPAC14)* (2014) pp. 1165–1167.

[13] Fermilab Redmine, Nonlinear integrable optics in IOTA, `https://cdcvs.fnal.gov/redmine/projects/nio-dn` (2020), [Online; accessed 21-Oct-2020].

[14] N. Kuklev, pyIOTA, `https://github.com/nikitakuklev/pyIOTA` (2020), [Online; accessed 21-Oct-2020].

[15] *Proceedings of the 2019 North American Particle Accelerator Conference (NAPAC19)* (2019).